Pollen-based biome reconstructions over the past 18,000 years and atmospheric CO2 impacts on vegetation in equatorial mountains of Africa

Kenji Izumi, Anne-Marie Lézine

Pollen-based biome reconstructions over the past 18,000 years and atmospheric CO_2 impacts on vegetation in equatorial mountains of Africa

Izumi, K. [1,2], Lézine, A.-M.[3]

[1] Laboratoire de Météorologie Dynamique, IPSL, CNRS, Université Pierre et Marie Curie, 4 place Jussieu, 75005 Paris, France

[2] Laboratoire des Sciences du Climat et de l'Environnement, CNRS-CEA-UVSQ, Université Paris-Saclay, Gif-sur-Yvette cedex 91191, France

[3] Sorbonne Universités, UPMC, Paris 06 Université, CNRS-IRD-MNHN, Laboratoire LOCEAN/IPSL, 4 place Jussieu, 75005 Paris, France

10 **Abstract**

11 This paper presents a quantitative vegetation reconstruction, based on a biomization
12 procedure, of two mountain sites in the west (Bambili; 5°56′ N, 10°14′ E, 2273 m) and east
13 (Rusaka; 3°26′ S, 29°37′ E, 2070 m) Congo basin in equatorial Africa during the last 18,000
14 years. These reconstructions clarify the response of vegetation to changes in climate,
15 atmospheric pressure, and CO_2 concentrations. Two major events characterize the biome changes
16 at both sites: the post-glacial development of all forest biomes ca. 14,500 years ago and their
17 rapid collapse during the last millennium. The rates of forest development between the biomes
18 are different; a progressive expansion of lowland biomes and an abrupt expansion of montane
19 biomes. The trends of pollen diagrams and biome affinity scores are not always consistent in
20 some periods such as the Younger Dryas interval and end of the Holocene Humid Period,
21 because the biomization method is not a simple summarization of the pollen data, but also takes
22 biodiversity into consideration.

23 Our sensitivity experiment and inverse-vegetation modeling approach show that changes
24 in atmospheric CO_2 concentration unequally influence vegetation in different local
25 environments. The study also suggests that the biome changes prior to the Holocene result from
26 both changes in the atmospheric CO_2 concentration and climate. The development of warm-
27 mixed forest from xerophtic vegetation results from increases in atmospheric CO_2 concentration
28 and near-surface air temperature. Difference in local dryness results in the different biome
29 distributions, with more forest-type biomes at Bambili and more grass/shrub-type biomes at
30 Rusaka.

31 **1. Introduction**

Equatorial forests have been considered to be the most stable ecosystems on Earth. From the viewpoint of their great floral and faunal diversity, they must have been in existence over the last several million years even though their extent could have fluctuated with climate and atmospheric composition. However, some previous palaeoecological studies (e.g., Maley and Brenac, 1998; Vincens et al., 1999; Runge, 2002; Lézine et al., 2013a, b; Desjardin et al., 2013) show that the equatorial forest ecosystems in Africa have undergone drastic modifications (floristic, structural and palaeogeographic) in response to climate changes since the last glacial maximum (LGM, ca. 21,000 years ago, 21 ka). These modifications include the possible fragmentation of equatorial forested communities (Maley, 1996), the expansion of species restricted to high elevations today (Dupont et al., 2000) at the LGM and the collapse of the forests around 4-2 ka (Vincens et al., 1999; Lézine, 2007; Marchant and Hooghiemstra, 2004; Lézine et al., 2013a,b). Changes in plant distribution and abundance from the last glacial onwards were also observed in the lowlands all over North Africa, from the Equator to the Northern Tropic (e.g., Lézine et al., 2009; Watrin et al., 2009; Hély and Lézine, 2014). Moreover, ^{13}C measurements on leaf waxes implied the replacement of tropical montane forest by scrub vegetation, the downward migration of alpine treelines and the marked shift towards C4-plant dominance in the tropics during the last glacial period (e.g., Street-Perrott et al., 1997; Huang et al., 1999).

Climate factors, such as moisture and heat are commonly invoked to explain the changes in ecosystem composition and structure (e.g., Lézine et al., 2011; Anadón et al., 2014). Other factors, such as atmospheric pressure and atmospheric CO_2 could potentially also have some impacts on the vegetation through physiological processes. Reduced partial pressure of CO_2 and O_2 associated with an increase in altitude related to lower sea level during glacial times could

55 influence photosynthesis (e.g. Friend and Woodward, 1990; Terashima et al., 1995; Sakata and
56 Yokoi, 2002). A decrease in atmospheric CO_2 generally results in a reduction of in the
57 abundance of plants with C3-photosynthesis pathway because of the required increased rates of
58 photorespiration, and an expansion of C4-plants due to their adaptation anatomically and
59 physiologically to low atmospheric CO_2 concentrations (e.g., Ehleringer et al., 1997; Cowling
60 and Sykes, 1999). Simulations with the BIOME3 equilibrium vegetation model also indicated
61 that low atmospheric CO_2 alone could result in the observed replacement of tropical montane
62 forest by scrub vegetation at the LGM (Jolly and Haxeltine, 1997). To understand vegetation
63 changes at tropical high-elevation sites in paleoecological context, we therefore need to
64 understand the effect of changes in the atmospheric CO_2 concentration and air pressure to the
65 vegetation as well as purely climatic effects.

66 In this study we focus on changes in biomes at roughly similar altitude (2000~2300 m) in
67 tropical Africa: to the West in the Cameroon volcanic line (Bambili) and to the East in the Kivu
68 montane range (Rusaka). Detailed pollen studies at both sites (Lézine et al., 2013a**;** Bonnefille et
69 al., 1995) have shown that vegetation composition varied considerably through time from 18 ka
70 to the present. The goals of our paper are 1) to discuss biome changes in these mountain areas
71 over the past 18 ka and 2) to investigate the impacts of changes in atmospheric CO_2
72 concentration on vegetation at the early in the last deglaciation (i.e., 18 ka) using an inverse
73 vegetation-modeling approach. The comparison between two distant sites will enable us to
74 identify the more prominent climate-change events that have affected the Afromontane forests.

75 **2. Equatorial mountains of Africa**

76 **2.1 Geographical features**

The Cameroon volcanic line is a crescent-shaped chain of highlands and volcanoes that extends from the Gulf of Guinea to the Southwest to the Adamawa plateau to the Northeast. Mean altitude decreases from West (around 2000 m in the "Grassfield" region) to East (around 1000 m in the Adamawa plateaus), punctuated by high mountains, such as Mount Cameroon on the coastline (4095 m) and Mount Oku in the Western plateaus (3011 m). Bambili is a crater lake located in the Western plateaus (05°56′ N, 10°14′ E, 2273 m; Figure 1) close to Mount Oku where the Afromontane forest is preserved today (Letouzey, 1968, 1985; Momo Solefak, 2009). Regional precipitation, with the rainy season from March to October, is due to the West African monsoon. The temperature is lower relative to lowlands over the tropical Africa due to the altitude of the site.

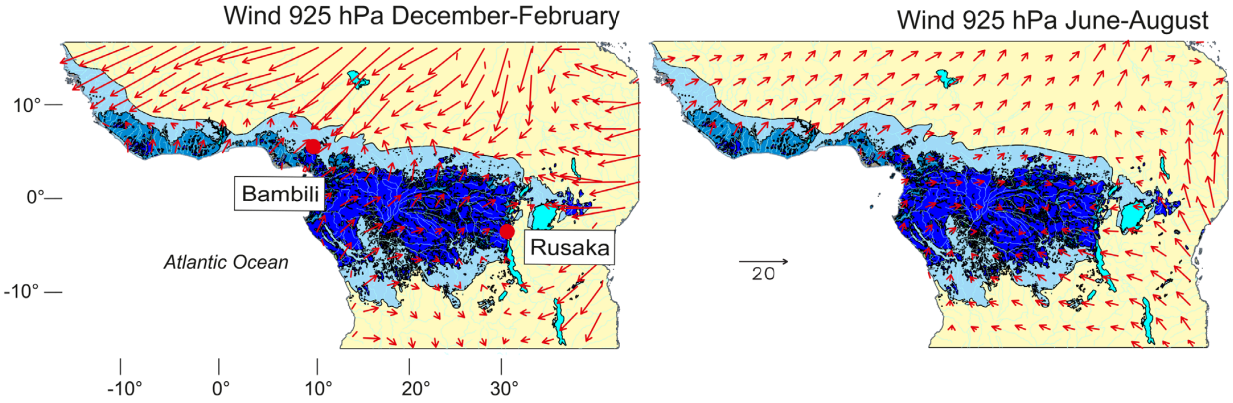

Figure 1. Location of the two pollen sites: Bambili (Lézine et al., 2013a) and Rusaka (Bonnefille et al., 1995); Guineo-Congolian forests (blue): rain forest (dark blue), deciduous forests (medium blue) and mosaic of forest and savanna (light blue). Sudanian, Zambezian savannas, Sahelian and Somalia-Masai steppes and deserts (yellow) (White, 1983). Arrows indicate the direction of main wind flow at 925 hPa in winter (left) and summer (right).

The Burundi highlands are a part of the Albertine Rift Mountains that enclose the western branch of the East African Rift, following a roughly North-South direction. The mountain ranges include high mountains, such as the Virunga Mountains (4507 m) and the Rwenzori Mountains (5109 m). These altitudes are not reached in Burundi where the highest peak reaches 2684 m only. Rusaka is a swamp lying at 3°26' S, 29°37' E and 2070 m in altitude (Figure 1). The

regional climate of Rusaka is related to the South African monsoon, the rainy season is from November to May.

2.2 The African biomes

Fossil pollen data are generally expressed in the form of abundances of individual plant taxa, and detailed pollen descriptions at Bombili and Rusaka have been provided elsewhere (Bonnefille et al., 1995; Lezine et al., 2013). The pollen sequence is continuous and extends from 0 to 18,071 years ago at Bambili and extends from 750 to 18,061 years ago at Rusaka. Here we use biomes, which are geographically and climatically broadly distributed physiognomic vegetation types, for representing vegetation changes in this study. The biomes are represented by assemblages of plant functional types (PFTs) that are defined on the basis of plant traits (e.g., the life form, leaf form, phenology, and bioclimatic tolerances) that reflect their preferable environments, in which the species maximize productivity and minimize environmental stress (Table 1). The use of biomes and PFTs helps to solve the problem of classifying paleoecological records by reducing the number of entities considered and by proving an ecological basis for treating plants from different regions in a comparable way. A method for converting pollen taxa to biomes (i.e. biomization) is described in section 3.1.

Table 1. Plant functional types proposed for the west and east African areas

PFT	
te	Tropical evergreen
tr1	Wet tropical raingreen
tr2	Dry tropical raingreen
tr3	Driest tropical raingreen
sf	Steppe forb/shrub
df	Desert forb/shrub

wte1	Warm-temperate broad- and needle-leaved evergreen (higher elevation)
wte2	Warm-temperate broad- and needle-leaved evergreen (lower elevation)
c3a	C3 herb from lowlands areas at the boundary between the Saharan and the Mediterranean zones
c3b	C3 herb from the afroalpine grasslands (top of the mountains >2800m alt)
c4	C4 herb (tropical grasslands and savannas)

The Afromontane vegetation of Africa is discontinuous, with patches separated from one other by lowlands, and thus is referred to as the "Afromontane archipelago" (White, 1983). Despite the geographic discontinuity, they share numerous plant species that are distinct from the surrounding lowland regions. Three main biomes (Table 2), common to all Afromontane regions, are distinguished. They correspond to an elevation gradient from roughly 1600 m to the top of the highlands:

- Warm mixed forest (WAMF) occurs in a lower ombrophilous areas and in the lowland Guineo-Congolian forests;
- Afro-alpine forest (AAF) occurs in an areas at higher elevation typically above 2000 m, with upper limit of the forest is typified by the presence of abundant Ericaceae; and
- Afro-alpine grassland (AAG) is cool afro-alpine grasslands that consist of C3 grasses which are found neR the top of the mountains above 2800 m.

Regional differences between the eastern and western mountain ranges are observed, however, with e.g., *Hagenia*, *Clifforita*, *Afrocrania* and *Junioerus* absent from the western sector (Cameroon), as well as *Artemisia* that has never been collected here.

131 **Table 2**. West and east African biomes and their characteristic plant functional types (PFTs),
132 main phytogeographical affinities and main vegetation types (White, 1983)

Biomes	PFTs	main phytogeographical affinities	main vegetation types (main taxa *)
AAG	c3b	Afromontane archipelago-like centre of endemisms (VIII)	Afromontane udifferentiated montane vegetation (C3 grasses mainly Poaceae, *Alchemilla*, Asteraceae)
AAF	wte1	Afromontane archipelago-like centre of endemisms (VIII)	Afromontane udifferentiated montane vegetation (*Podocarpus*, *Prunus*, *Syzygium*, *Nuxia*, *Rapanea*, *Maesa*, *Myrsine*, *Hagenia*, *Juniperus*, *Hypericum,* Ericaceae)
WAMF	wte2	Afromontane archipelago-like centre of endemisms (VIII)	Afromontane udifferentiated montane vegetation (*Podocarpus, Ilex, Schefflera, Syzygium, Olea, Strombosia, Ficus, Celtis,* Rutaceae, Sapindaceae, Euphorbiaceae)
TRFO	te	Guineo-Congolian regional center of endemism (I)	Lowland rain forest: wetter types (Caesalpiniaceae, Mimosaceae, Moraceae, Meliaceae, Irvingiaceae)
TSFO	tr1	Guineo-Congolian regional centre of endemism (I)/ Guineo-Congolian/Sudanian/Zambezian regional transition zone (XI)	Lowland rain forest: drier types / mosaic of lowland rain forest and secondary grassland / Swamp forest (Ulmaceae, Sterculiaceae)
TDFO	tr2	Sudanian (III)/Zambezian (II) regional centre of endemism	Woodland / dry forest / Miombo (*Brachystegia*, *Julbernardia*, *Isoberlinia*, Combretaceae, *Lannea*, *Prosopis*, *Hallea*, *Monotes*, *Protea*, Euphorbiaceae.)
SAVA	tr3+c 4	Southern Sahel regional transition zone (XVI)/Guineo-Congolian/Sudanian regional transition zone (XI) – Zambezian transition zone (X)/Lake Victoria mosaic (XII)	Wooded grassland/ deciduous bushland/ mosaic of lowland rain forest and secondary grassland (C4 tall (up to 3m high) grasses, *Terminalia*, *Lophira*, *Mitragyna inermis*, *Borassus aethiopium*)
STEP	sf+c4	Northern Sahel regional transition zone (XVI)/Somalia-Masai regional centre of endemism (IV)	Semi-desert grassland and shrubland (C4 short grasses, *Acacia*, *Commiphora*, *Balanites*, Capparidaceae)
DESE	df+c4 +c3a	Sahara regional transition zone (XVII)	Desert (C4 short grasses, Chenopodiaceae/Amaranthaceae, Resedaceae, Brassicaceae)

133 * Pollen nomenclature follows Vincens et al. (2007).
134

135 Lowland African biomes (Table 2) are distributed along a decreasing rainfall gradient
136 from the Guineo-Congolian forests, which ranges from tropical rain forest (TRFO) and tropical
137 seasonal forest (TSFO) (near the Equator), to the Sudanian (to the North)/Zambezian (to the East

and South) tropical dry forests (TDFO), to a mixture of woodlands and grasslands (i.e. savanna (SAVA)), to the Sahelian (to the North)/Somalia Masai (to the East) steppes (STEP), and finally to desert (DESE).

In this study, we focus on nine biomes (three biomes for highlands and six biomes for lowlands) on the basis of our own field expertise and local descriptive botanical literature (Troupin, 1982; Letouzey, 1968, 1985; Momo Solefak, 2009).

3. Methods

3.1 Biomization procedure

Biomization is a quantitative procedure that reconstructs biomes on the basis of the characteristic signature in the pollen record of different PFTs (Prentice and Webb, 1998). There are five steps in the biomization method used here: (1) assignment of taxa represented in the pollen assemblages to PFTs (i.e., defining a taxon × PFT matrix), (2) definition of biomes as combinations of PFTs (defining a PFT × biome matrix), (3) combination of the above two matrices (defining a taxon × biome matrix by simple matrix multiplication of the matrices from steps 1 and 2), (4) for a particular pollen assemblage, calculation of affinity scores for each biome, and (5) selection of a biome with the highest affinity score as the dominant biome represented by that pollen assemblage. The detailed formula for step 4 is described in Prentice and Webb (1998). The affinity score for each biomes can be thought of as a measure of the likely presence at a site of that biome given the particular pollen spectrum, such that the lower affinity the score, the less likely the biome is to be present. The score is not equivalent to the proportion of the area covered by an individual biome at the site, but simply describes presence or absence.

159 The biomization procedure has been successfully used worldwide to reconstruct modern
160 and past biomes for selected time periods, typically the last glacial period and the Holocene (e.g.
161 Prentice et al., 2000; Elenga et al., 2000; Jolly et al., 1998a). Within tropical Africa, the method
162 has been applied to modern pollen samples at the continental scale (Jolly et al., 1998) or more
163 regionally in East (Vincens et al., 2006) and West Africa (Lézine et al., 2009). Past biome
164 reconstructions have also been performed for Plio-Pleistocene (Bonnefille et al., 2004; Novello
165 et al., 2015) and more recent (from the last glacial to the present) sections (Lebamba et al., 2012;
166 Amaral et al., 2013).

167 We have used the complete matrices, pollen taxa-PFTs-biomes for both Bambili and
168 Rusaka defined by Vincens et al. (2006) and Lézine et al. (2009), respectively, and the PFTs-
169 biomes matrix (Table 1, 2) is the same for both sites. The lakeshore aquatic plant taxa and ferns
170 taxa were removed as these respond to local hydrological conditions, rather than being reflective
171 of broader scale climate controls. While a 0.5 % threshold for all taxa has generally been used in
172 calculating affinity scores to reduce the incidence of misassignment among relatively species-
173 poor assemblages (Prentice and Webb, 1998), we selected 0.2 % threshold for this study after an
174 examination of several biomization practices. We also used a threshold (40%) for Poaceae in
175 order to minimize the over-representation of this taxon in individual pollen spectra.

176 **3.2 A sensitivity experiment for a simple CO_2 effect on vegetation**

177 In order to explore the impact of change in atmospheric CO_2 alone on vegetation at
178 Bambili and Rusaka, we first performed a sensitivity experiment. The experimental design is
179 similar to the one in Jolly and Haxeltine (1997); the observed seasonal climate data is held
180 constant and only atmospheric CO_2 concentration is varied (from 400 ppm to 180 ppm, 10 ppm

interval) for running two coupled biogeography and biogeochemical models, BIOME5-beta (Izumi, 2014) and BIOME4 (Kaplan et al., 2003). These models simulate common equilibrium vegetation and bioclimatic variables, but they have different vegetation responses to change in atmospheric CO_2 concentration (e.g., BIOME5-beta has lower carbon use efficiency, the ratio of net primary production to gross primary production). In running these vegetation models, we use monthly climate from CRU CL 2.0 (New et al., 2002) and soil (FAO, 1995) at each site. Altitude-adjusted air pressure is used at each site (7.7×10^4 Pa at Bambili and 7.9×10^4 Pa at Rusaka).

3.3 Inverse-modeling through an iterative forward modeling approach

In order to examine the potential impacts of altitude and changes in atmospheric CO_2 concentration on vegetation from the viewpoint of pollen-based climate reconstruction, we used an "inverse modeling through iterative forward modeling" (IMIFM) approach (Izumi 2014; Izumi and Bartlein, in revision), which can be compared with the forward modeling approach that uses inputs of climate and CO_2 concentrations to mechanistically simulate vegetation. The IMIFM approach (also called "inverse vegetation modeling" approach for climate reconstruction in Guiot et al. (2000) and Wu et al. (2007a)), was developed to overcome some disadvantages of conventional statistical reconstruction approaches, such as modern-analogue, regression, and response-surface techniques. These conventional approaches generally require several ecological assumptions for climate reconstruction from pollen data, in particular that climate is the ultimate cause of change in vegetation, and the modern data contain all the information necessary to interpret the paleodata (Guiot et al., 2009). However, plant-climate interactions are very sensitive to atmospheric CO_2 concentration (e.g., Cowling and Sykes, 1999; Prentice and Harrison, 2009)

and thus modern pollen samples influenced by higher CO_2 concentrations of the past century are not necessarily good analogs for climates under lower CO_2 concentrations.

The basic assumption of the IMIFM approach is that it should be possible to reconstruct the climate data that gave rise to a "target" paleovegetation sample by searching for the set of climate scenarios, which input to a forward vegetation model yields a simulated vegetation that resembles the vegetation represented by a target fossil-pollen sample. The application of the IMIFM approach involves the generation of many thousands of candidate sets of individual climate-variable values that are individually discarded or retained depending on their ability to correctly generate the observed vegetation using a specific forward model. The retained climate-variable values, which allow a correct simulation of the target vegetation, are then statistically summarized to provide the reconstructed or estimated values of the climate variables.

The IMIFM approach has the potential to provide more accurate quantitative climate estimates from pollen records than statistical approaches because it allows the mechanistic effects of non-climatic variables, such as the atmospheric CO_2 concentration and atmospheric pressure, to be explicitly considered in the reconstruction. However, the approach is strongly dependent on the quality of the forward vegetation model. Therefore, to reduce the dependency of our results on a single model, we use two equilibrium vegetation models, BIOME5-beta and BIOME4. The detailed methodology and vegetation models consulted for individual papers.

In the IMIFM approach for climate reconstruction, we need to compare pollen-based observed biomes with the simulated biomes in the vegetation models. We define the simulated biomes as follows: the afro-alpine forest (AAF) is composed of simulated scrubland and mixed forest, and the afro-alpine grassland (AAG) is the simulated temperate grassland, but the climate

225 spaces for both AAF and AAG are based on the climatic requirements of temperate
226 microphyllous shrub vegetation (i.e., the minimum mean temperature of the coldest month
227 (MTCO) is 5 °C, and the maximum of the MTCO is 10.5 °C) in Jolly et al. (1998b). The climate
228 spaces for simulated warm mixed forest (WAMF) are based on BIOME4's description of
229 WAMF, but the minimum of MTCO is increased to 10.5 °C. Below that threshold in MTCO the
230 simulated biome is regarded as AAF. In searching the climate scenarios over the deep tropical
231 areas, we allow for differences between mean temperature of the warmest month (MTWA) and
232 MTCO of less than 7 °C.

233 In order to investigate the effects of changes in atmospheric CO_2 concentration to climate
234 spaces of a target biome (i.e., AAF at Bambili and AAG at Rusaka) at the early in the last
235 deglaciation (i.e., 18 ka), we set two experiments using the IMIFM approach at each site; exp. 1)
236 paleo atmospheric CO_2 concentration (194 ppm for ca. 18 ka; Bazin et al., 2013) and exp. 2)
237 modern atmospheric CO_2 concentration (331 ppm). The difference between exp.1 and exp. 2
238 shows the effects of atmospheric CO_2 difference to the target biome. In running these vegetation
239 models, we use monthly climate from CRU CL 2.0 (New et al., 2002) and soil (FAO, 1995) at
240 each site. Altitude-adjusted air pressure is used at each site (7.7×10^4 Pa at Bambili and $7.9 \times$
241 10^4 Pa at Rusaka).

242 **4. Results**

243 **4.1 Vegetation changes**

244 First, we present summary pollen diagrams showing percentages of the three main pollen
245 groups: trees, herbs and undifferentiated (which correspond to pollen grains determined at a too
246 low taxonomic level and/or pollen grains corresponding to plants with a variety of life forms) in

order to illustrate the main physiognomical changes (i.e., ratio between trees and herbs) over the last 18 ka at Bambili and Rusaka (Figure 2a-b). Both sites have varying degrees of vegetation change, but the pollen percentages show some common trends between the two sites over the last 18 ka; a progressive expansion of forests over the last glacial-interglacial transition period, in particular during the Bølling/Allerød warm period (ca. 13.8 ka) and the Holocene, and degradation of the forests during the Younger Dryas interval (ca. 12.9 to 11.7 ka), and at ca. 8.2 ka, 3.3 ka, and 1.2 ka.

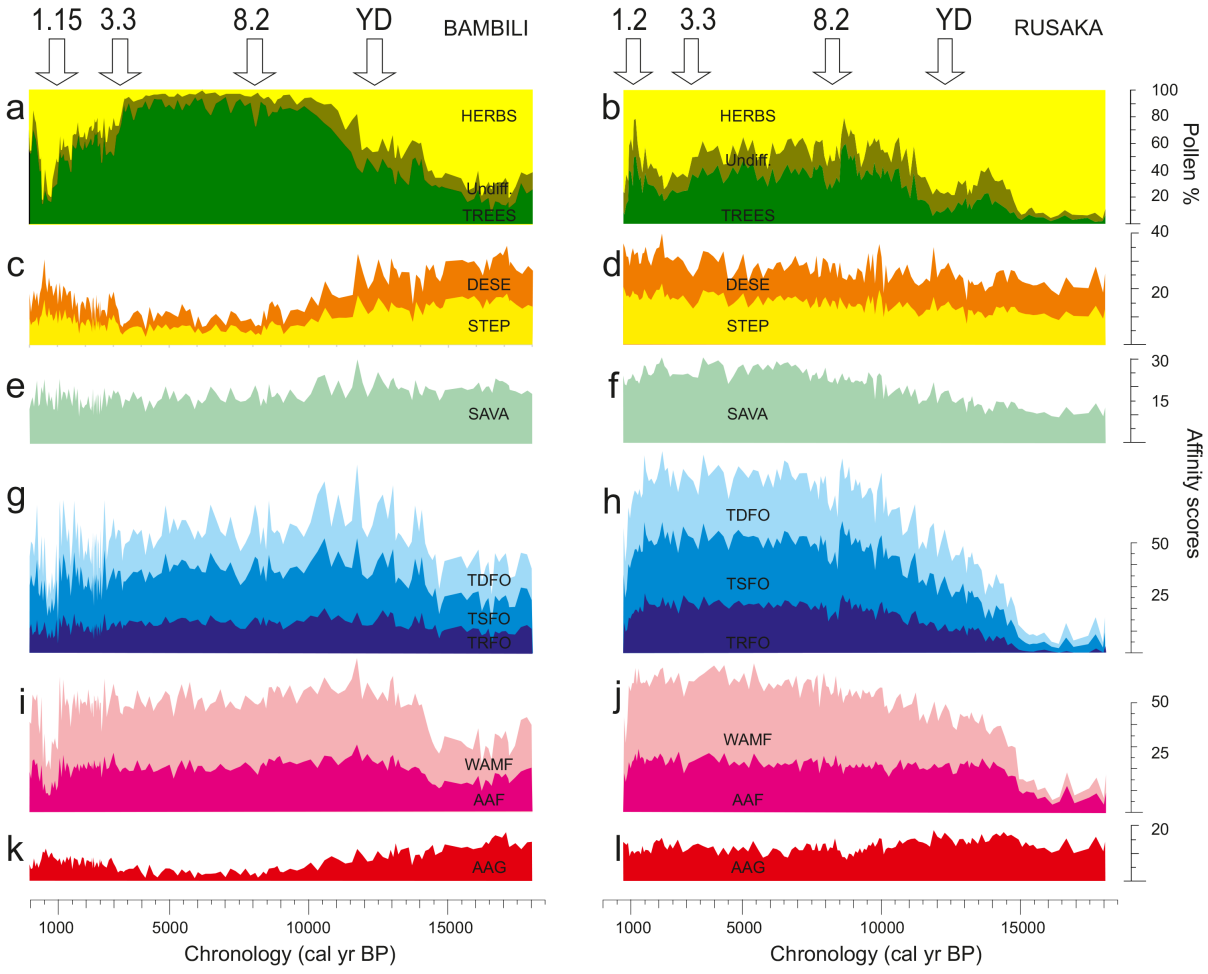

Figure 2. Synthetic pollen diagrams (trees, herbs and undifferentiated; a-b) and affinity scores of each biome (c-l) at Bambili and Rusaka.

Next, we show each biome score over the last 18 ka at both sites (figure 2c-l). These biome scores are a measure of the likely presence of the biome; both highland (afro-alpine forest (AAF) and warm mixed forest (WAMF)) and lowland (tropical rain forest (TRFO), tropical seasonal forest (TSFO) and tropical dry forest (TDFO)) forest biomes show relatively high affinity scores through the entire period at Bambili (Figure 2g and 2i). From 18 ka, they increased, through fluctuating, to an optimum that they reach at ca. 14.5 (for the AAF and WAMF) and 10.3 ka (for the TRFO, TSFO and TDFO) during the last deglaciation. The highest affinity scores of all these forest biomes are reached during the phase of developing forests (ca. 11.5 ka) according to the pollen diagram (Figure 2a). During the Holocene, in contrast to the relative stability of the montane forest biomes, affinity scores of lowland forests ones decreased from ca. 10.3 ka onward. While they remained relatively stable in spite of a period of slight decline from ca. 4.7 to ca. 1.15 ka, the 3.3ka event (the significant fall of tree pollen percentage) is not recorded in our forest biome reconstructions. On the contrary, all the forest biomes abruptly collapsed at ca. 1.15 ka as shown by the dramatic fall of their cumulative scores, of 50% within ca. 70 years only. It was only after ca. 0.5 ka that forest biomes recovered and then reached their Holocene affinity-score values (Figure 2g and 2i).

The open grass/shrubland biomes (afro-alpine grassland (AAG), steppe (STEP) and desert (DESE)) progressively diminished from ca. 18 ka to ca. 8.2 ka, and then gradually increased until the present at Bambili (Figure 2c and 2k). The higher affinity scores of some xerophytic biomes (STEP and DESE) at ca. 3 and ca. 1.15 ka are also consistent with the herb pollen percentage (Figure 2a and 2c). The trends of these biome scores are similar to the trend of herb pollen percentages. On the other hand, the affinity score of savanna (SAVA) was relatively high throughout the whole period (Figure 2e).

The time interval between ca. 18 and ca. 15 ka had unfavorable conditions for tropical lowland forests (TRFO, TRSO, and TDFO) and montane forests (AAF and WAMF) at Rusaka (Figure 2h and 2j). The tropical lowland forests started to develop at ca. 14.5ka and then progressively increased until ca. 8.5 ka. After the forest expansion was abruptly interrupted between ca. 8.5 and ca. 8 ka, the lowland forests remained stable until ca. 1.5 ka. On the other hand, the montane forests abruptly increased at ca. 15 ka, then followed different trends: in contrast to the AAF which remained stable, the WAMF continuously expanded until ca. 4 ka and then remained relatively stable until ca. 1 ka. Among all the phases of forest decrease which punctuated the African Humid Period (ca. 9 ka to ca. 6 ka), only that corresponding to the 8.2 ka event is clearly reflected by the sharp decrease of he scores of all the lowland forest biomes. The tropical lowland forests and WAMF recorded a dramatic decline during the last few hundred years.

The affinity scores of xerophytic biomes (AAG, STEP, DESE and SAVA) are higher than those for forest biomes during the period between ca. 18 ka and ca. 15 ka, which is consistent with the pollen percentages at Rusaka (Figure 2b, 2d, 2f and 2l). The affinity scores of the xerophytic biomes did not largely change through the entire period, but there is an opposite trend between highlands and lowlands: the AAG progressively decreases and the other biomes progressively increase from the glacial period to the present. The Holocene evolution of SAVA, STEP and DESE was punctuated by phases of slight reduction at ca. 12, 10.5, 3.7-3.2, and 2.1 ka.

Figure 3 shows the first and second dominant biomes for representing the main biome changes at Bambili and Rusaka sites. We chose a biome with the highest affinity score as the first dominant biome and a biome with the next highest score as the second dominant one. The

higher ratios of the second dominant biome affinity score to the first dominant biome affinity score express the potential co-existence of these biomes. The first dominant biome over the Holocene is the warm-mixed forest (WAMF), which is in particular the sole dominant biome except ca. 1 ka and ca. 9 ka, and it has relatively high affinity scores at both sites, but there are different biome distributions and have lower affinity scores (than the Holocene) between the two sites prior to the Holocene. The WAMF was already the first dominant biome from ca. 15 ka, and before the establishment of the forest, savanna (SAVA) was the first dominant biome at Bambili. On the other hand, the WAMF was first dominant biome from ca. 13 ka, and before the forest establishment, afro-alpine forest (AAF, ca. 15 ka to ca. 13 ka) and afro-alpine grass (AAG, ca. 18 ka to ca. 15 ka) was the first dominant biome at Rusaka.

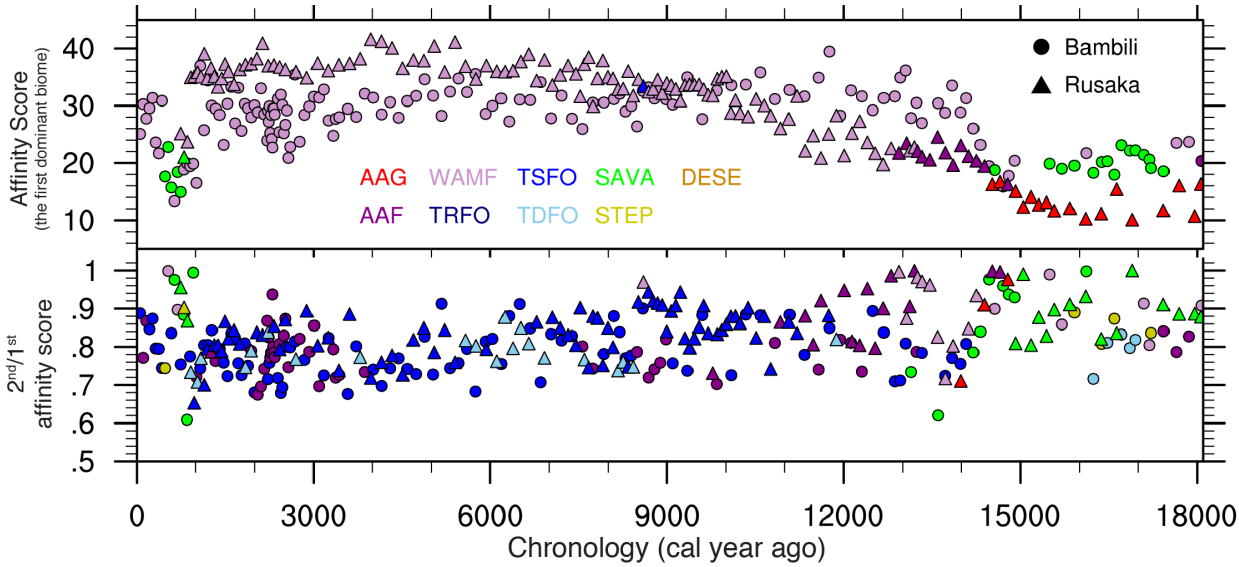

Figure 3. The first and second dominant biomes and their affinity scores at Rusaka and Bambili. The first dominant biome affinity score is shown with the absolute value (top). The affinity scores of the second dominant biomes are shown with the ratio of the second biome affinity score to the first biome one (bottom).

4.2 Effects of atmospheric CO_2 concentration to vegetation

Unlike the sensitivity experiment in Jolly and Haxeltine (1997), our sensitivity experiment does not show a shift of the warm mixed forest (WAMF) to the target xeric biomes

(afro-alpine forest (AAF) at Bambili and afro-alpine grassland (AAG) at Rusaka) by the decreases in atmospheric CO_2 alone (not shown). But, under the lower CO_2 concentrations, the simulated net primary production (NPP) largely decreases for most of the forest-related plant functional types (PFTs) and slightly decreases for shrub- and grass-related PFTs (Fig. 4). The sensitivity analysis thus shows that the xerophytic biomes have relatively higher NPP and thus more easily expand than forest biomes under lower atmospheric CO_2 concentrations. To a greater or lesser extent, these responses are consistent among the BIOME models (i.e., BIOME3, BIOME4, and BIOME5-beta).

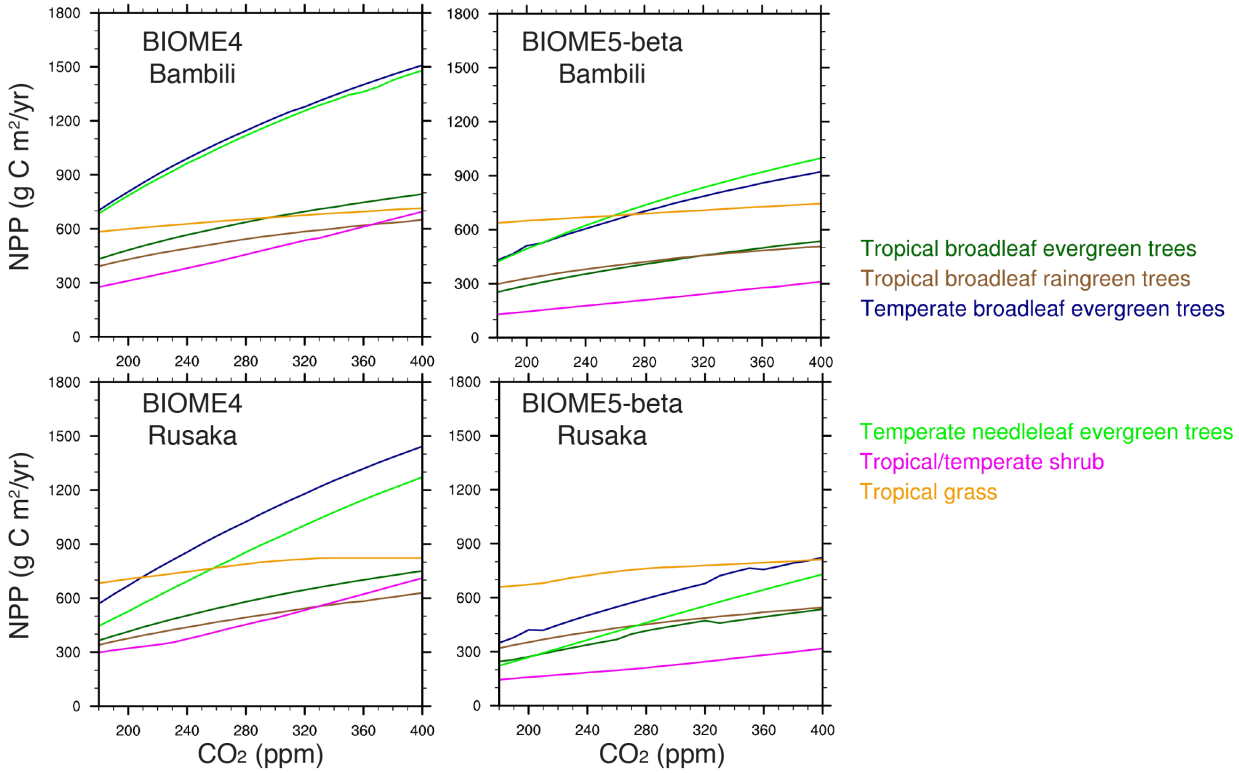

Figure 4. Change in net primary production (NPP) in the sensitivity experiment. In running the vegetation models (i.e., BIOME4 and BIOME5-beta), we use the altitude-adjusted air pressure (7.7×10^4 Pa at Bambili, 7.9×10^4 Pa at Rusaka). The climate input comes from CRU CL 2.0 data at each site.

To illustrate the possible climate spaces for target vegetation (i.e., AAF at Bambili and AAG at Rusaka) under the different atmospheric CO_2 concentration, we estimated mean annual

temperature (MAT, °C) and mean annual precipitation (MAP, mm/year) using the IMIFM approach with both BIOME5-beta and BIOME4 vegetation models (Fig. 5). This target vegetation is the observed first dominant biome, which has the highest affinity score, at the early in the last deglaciation (i.e., 18 ka) (the rightest part in Fig. 3). According to observed climate data, CRU CL 2.0 (New et al., 2002), although MAT is similar at both sites, MAP at Rusaka is less than half at Bambili (Figure 5), and thus Rusaka is likely to experience drier conditions than Bambili for vegetation at both the present and past.

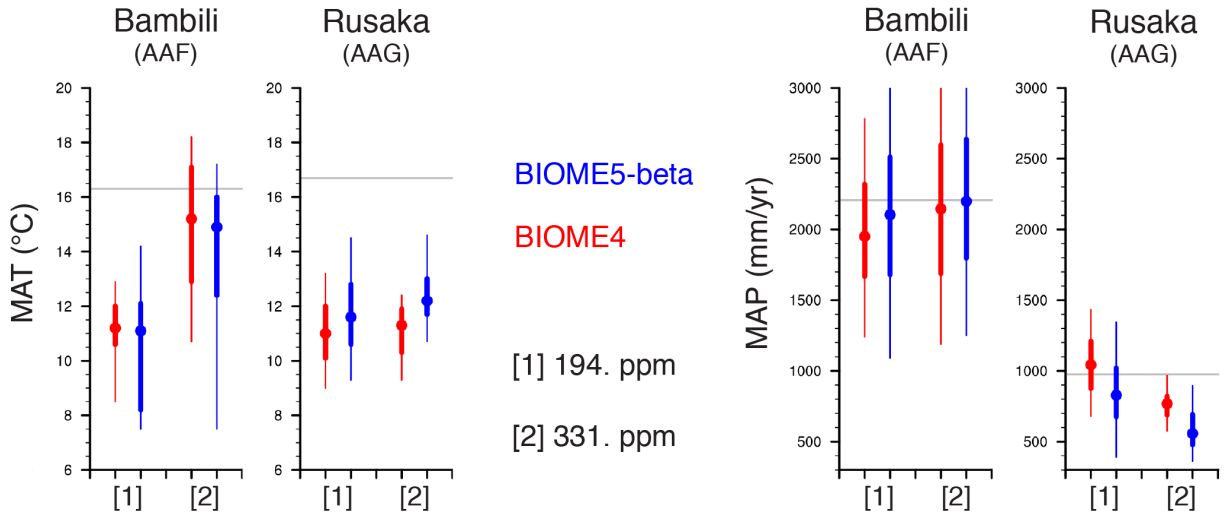

Figure 5. Potential climate (mean annual temperature (MAT) and mean annual precipitation (MAP)) spaces for target vegetation (i.e., afro-alpine forest (AAF) at Bambili and afro-alpne grass (AAG) at Rusaka) at ca. 18 ka (18,071 years ago at Bambili and 18,061 years ago at Rusaka) using the IMIFM approach with two vegetation models through two experiments: [1] paleo CO_2 concentration (194. ppm) and [2] modern CO_2 concentration (331. ppm). Dots indicate median values, bold vertical lines indicate interquartile intervals (25^{th} to 75^{th} percentile), and thin vertical lines indicate 90 % interval (5^{th} to 95^{th} percentile) for probability distribution of each climatic variable from BIOME5-beta (blue) and BIOME4 (red) respectively. The gray lines indicate observed modern values from the CRU CL2.0 (New et al., 2002) data at each site.

The difference of atmospheric CO_2 concentration (i.e., 331 ppm at 0 ka vs. 194 ppm at ca. 18 ka) also influences plant productivity and climate spaces for the target vegetation (i.e. AAF at Bambili and AAG at Rusaka) (Figure 5 [1] and [2]). The change in atmospheric CO_2 level (i.e., from 331 ppm to 194 ppm) decreases the simulated GPP, AR, and NPP by 30-45% at

Bambili with both vegetation models, but changes in these variables are different between the vegetation models at Rusaka; BIOME4 shows a greater response than the BIOME5-beta related to the different carbon-use efficiency simulation between models. At Rusaka, BIOME5-beta slightly increases in AR and decreases in both GPP and NPP, and there is different responses between grass-type biomes and woody-type biomes in the single model. Compared to the modern CO_2 experiment (Figure 5 [2]), the paleo CO_2 experiment (Figure 5 [1]) with both models shows that the MAT drops by around 4 °C and MAP decreases about 150 mm/year at Bambili, and that MAT drops about 0.5-1 °C and MAP increases about 200-300 mm/year at Rusaka. The response of the forest-type biome (i.e. AAF at Bambili) to the change in atmospheric CO_2 concentration is much larger than one of the grass-type biome (i.e. AAG at Rusaka).

5. **Discussion**

5.1 Vegetation changes

Inspection of the formula for calculating affinity scores in the biomization procedure, shows that the scores for each biome do not simply reflect the sum of pollen percentages that constitutes each biome. If the percentage of the pollen sum that constitutes each biome is fixed, greater diversity among taxa for a given biome will automatically yield a higher affinity score (Prentice and Webb, 1998). Therefore, the trends of pollen abundance and affinity scores will not necessarily be consistent even if we use the exact same pollen data (Figure 2). However, the general trend of forest expansion, forest establishment, and forest degradation described using both pollen percentages and biome scores at Bambili and Rusaka is mutually consistent here.

We also calculated other biome score ratios: AAG/AAF for implying the vertical migration of the tree line in mountains (Figure 6a), and TRFO/STEP (i.e., the most humid biome versus the one of the most arid biomes) for implying the lowland changes in biomes mainly linked to moisture changes (Figure 6b). AAG/AAF displays a parallel trend at both sites with high values at levels dated from 18 to 14.5ka. AAG/AAG values abruptly fall at 14.5 (Ruzaka) or 13.7ka (Bambili) then remain stable during the Holocene until the last millennium where a sharp increase is observed. Conversely TRFO/STEP values increase from 18 ka to 14.7 (Rusaka)-14ka (Bambili) with values substantially higher at Bambili compared to Rusaka. In this latter site, they remain stable during the Holocene, whereas the dramatically increase during the mid-and late Holocene at Bambili.

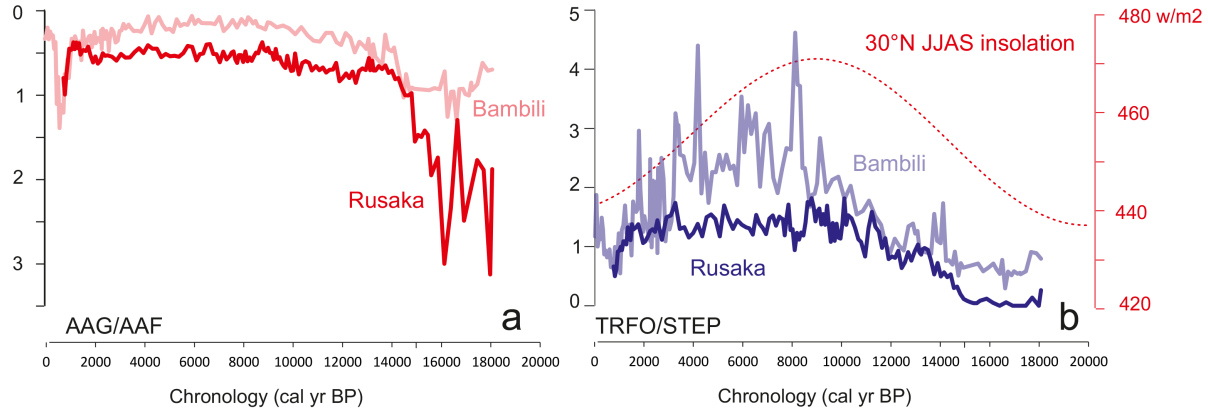

Figure 6. AAG/AAF ratio illustrating the descent of the tree line at Rusaka and Bambili (a) and TRFO/STEP ratio illustrating the expansion of the lowland forests in relation with increased humidity (b). 30 °N JJAS insolation from Berger and Loutre, 1991.

One of the remarkable results of our analysis is the characterization of the period prior to the Holocene forest establishment. The first dominant biome over the Holocene is the warm mixed forest (WAMF) at both Bambili and Rusaka, but the biome distributions were different between the two sites prior to the Holocene (i.e., WAMF and savanna (SAVA) at Bambili and AAF and afro-alpine grass (AAG) at Rusaka) (Figure 3). While the extreme reduction of all kinds of forests is coeval with both the expansion of the lowland grasslands and shrublands and

398 the downward shift of the Afroalpine grasslands (Figure 6a) during glacial times at Rusaka, such
399 a shrinkage was not observed at Bambili where all forest biomes were present at that time – even
400 with noticeable reduction of their population size – and where the downward shift of the
401 Afroapline belt was much less pronounced (Figure 6a)

402 Our result proposes that the eastern and western sectors of the Guineo-Congolian forest
403 domain had the following distinct environmental conditions: northwest Cameroon benefited from
404 conditions favorable to forest persistence at both low and high elevation in spite of dryness
405 related to Heinrich event 1 (H1, ca. 17 ka) (Stager et al., 2002). The forest domain was probably
406 not as fragmented as previously thought (Maley, 1996). Lower atmospheric CO_2 concentration
407 and regional dryness allowed for xerophytic biomes to expand in the lowlands. For some
408 vegetation, the impact of lower CO_2 concentration is equivalent to that of increased dryness
409 (Loehle, 2007). By comparison, the environment was too dry in the Burundi highlands for the
410 persistence of any kind of forests.

411 Atmospheric CO_2 concentrations over the Holocene were still lower than modern, but the
412 impact on the vegetation is generally considered to be negligible for practical purposes. Here, the
413 expansion of xerophytic biomes mainly results from increased dryness. As shown by the
414 TRFO/STEP ratio (Figure 6b), the expansion of moist forest biomes in the lowlands at both sites
415 closely matches the insolation trend (Braconnot et al., 2007a, 2007b) and related fluctuations in
416 monsoon rainfall since ca. 15 ka (e.g., deMenocal et al., 2000; Weldeab et al., 2005; Gasse et al.,
417 2000, 2008; Lézine et al., 2011; Tierney et al., 2008; Tierney and deMenocal, 2013). Unlike
418 Rusaka where the driest biomes continued into the Holocene, Bambili recorded a drastic decline
419 of STEP and DESE, which corresponded to the onset of the “African Humid Period” i.e the
420 widespread expansion of tropical forests and woodlands in northern Africa (deMenocal et al.,

2000; Lézine et al., 2011; Hély and Lézine, 2014). Moist conditions led to the progressive forest expansion in the lowlands as shown by the increase of their biome scores (Figure 2) during the period 15-8.5ka (the Younger Dryas (YD) interval excluded) contrary to WAMF, which abruptly developed within centuries. Then the WAMF dominated in the surroundings of the lake at both sites all along the Holocene (Figure 3).

The YD climate reversal is associated with an intense drought in the African tropics (Gasse et al., 2008), which was responsible for forest disruption (see the fall in tree pollen percentages, Figure 2) but that only slightly affected the biome distribution (Figure 2). This is confirmed by the only small decrease of the TRFO/STEP ratio (Figure 6b). In contrast, the 8.2 ka dry event (Alley, 1997) is particularly clear at Rusaka where the lowland forest biomes suddenly dropped (Figure 2). Moreover, the intrusion of TDFO as the second dominant biome after this event at this site (Figure 3) testifies for drier conditions in relation with a longer dry season as already observed in tropical Africa (e.g., Vincens et al., 2010). At Bambili however, diversity changes (an increase of light-demanding trees) induced by repeated dry seasons from ca. 8.2 ka onward (Lézine et al., 2013a) did not significantly affect the representativeness of the forest biomes, and the WAMF remained dominant up to the last millennium. An increase in drought at this site during the 8.2 ka event is only signaled by the higher scores of DESE and STEP.

The two-step disruption of the forest at the end of the African Humid Period at ca. 3.3 ka and then during the last millennium (Figure 2, tree pollen percentages) clearly corresponded to dry periods as shown by the increase of open grassland/shrubland biomes. The last millennium is by far the most disturbed period of all the late Holocene. The sudden decline of all the forest biomes at ca. 1.2 ka correlates the dry event already recorded in Equatorial Central (Brncic et al., 2009) and East Africa (Verschuren et al., 2000) at the time of the 'Medieval Warm Period'. One

444 cannot however exclude the role of human populations who widely expanded at that time
445 (Lézine et al., 2013b) in the forest degradation.

446 **5.2 Effects of atmospheric CO_2 concentration on vegetation**

447 Our study shows that changes in atmospheric CO_2 concentration impact on plant
448 productivity and vegetation distribution and thus possibly influence climate spaces for the
449 vegetation in equatorial mountains of African. These results are consistent with previous studies.
450 However, although Jolly and Haxeltine (1997) already proposed that low atmospheric CO_2 alone
451 could result in the observed replacement of tropical montane forest by scrub vegetation, this
452 dramatic change apparently depends on the local climate and vegetation model used. As a result,
453 whether the vegetation prior to the Holocene is due to lower atmospheric CO_2 concentration
454 relative to present, changes in the climate, or their combination is an unresolved question (Wu et
455 al., 2007b). Sensitivity experiments can be used to assess the impacts of a change in atmospheric
456 CO_2 concentration on vegetation, but it is difficult to consider the impacts of climate changes on
457 vegetation at the same time because similar vegetation can exist under a wide climate space.
458 Thus, the inverse-vegetation modeling approach (e.g., Wu et al., 2007a, b; Izumi and Bartlein, in
459 revision) can be one option for investigating impacts of changes in the atmospheric CO_2
460 concentration and climate on vegetation.

461 The changes in atmospheric CO_2 concentration potentially result in large impacts on
462 vegetation and climate reconstruction based on the vegetation in our sites. Our MAT estimation
463 at ca. 18 ka shows the similar values at Bambili and Rusaka because the target biomes are similar
464 afromontane biomes at the two sites. When we take into account modern MAT at each site, we
465 can therefore suggest similar temperature decreases at ca. 18ka in equatorial mountains of Africa.

466 According to our sensitivity experiment and IMIFM approach for climate reconstruction, the
467 vegetation changes from xerophytic biomes (afro-alpine forest (AAF) and afro-alpine grass
468 (AAG)) to warm mixed forest (WAMF) prior to the Holocene result from both the increase in
469 atmospheric CO_2 concentration and surface air temperature.

470 Our mean annual precipitation (MAP) estimation does not vary accompanying changes in
471 atmospheric CO_2 concentration in particular at Bambili, partly because of the impact of lower
472 CO_2 concentration on water-use efficiency (WUE; the ratio of rate of photosynthesis to the rate
473 of transpiration) in vegetation. If climate did not vary between the present and the past (at ca. 18
474 ka), the paleo vegetation in particular xerophytic biomes would still appear drier than present,
475 simply because of decreased WUE. WUE is sensitive to changes in atmospheric CO_2 through
476 effects on stomatal conductance, and consequently a decrease in WUE results from low CO_2
477 concentration (Lochle, 2007; Prentice and Harrison, 2009). Moreover, in spite of the similar
478 afromontane biomes at the two site, the MAP reconstructions are opposite between the two sites
479 because of the different WUE responses between forest-type and grass-type biomes to the lower
480 CO_2 concentration. This MAP increase at Rusaka also implies that climate reconstruction at ca.
481 18 ka would appear too dry if the decrease in atmospheric CO_2 concentrations was not
482 considered. There are different responses in plant productivity between AAG (at Rusaka) and
483 AAF (at Bambili) to a change in atmospheric CO_2 concentration (e.g., AAF has larger
484 responses), and this has a large impact on climate reconstruction but one that depends on the
485 vegetation models and vegetation types. The different types of biomes at Bambili and Rusaka
486 possibly result from both the regionally different dryness and the lower atmospheric CO_2
487 concentration.

Inverse-vegetation modeling approaches also have many challenges. One of the most significant issues is that the results depend on the vegetation model used (Guiot et al., 2009). In this study, we used the two equilibrium vegetation models, and there were some opposing responses between the models, and thus we need to further evaluate the models if we wish to produce robust results. Moreover, the inverse-vegetation modeling approach in Wu et al. (2007a, b) assumed that last glacial period was drier than the present and thus their potentially prescribed precipitation range was lopsided (i.e., -90% to 50% of modern values). But, if we do not have any evidence for the potential climate space (e.g. from lake-status data), we should search over a wider climate space (e.g., -90% to 90% of modern values) for the target vegetation.

6. Conclusion

Comparing two mountain sites located in different environments of equatorial Africa sheds some new light on the response of plant formation (i.e. biomes) to climate changes: (i) two major events characterize the changes biome distribution over the last 18 ka. Taking into account uncertainties of the age models, their timing is remarkably similar east and west of the Congo basin: the post-glacial development of all the forest biomes ca. 14.5 ka and their collapse during the last millennium; (ii) contrary to the lowlands where forests biomes expanded progressively, the montane forest development was abrupt, occurring within centuries. Mountain biomes then remained remarkably stable throughout the Holocene contrasting with the repeated fluctuations in the arboreal forest cover revealed by the tree pollen percentages. In particular, the forest decline during the Younger Dryas and at the end of the Holocene Humid Period at ca. 3.3 ka is not or only slightly reflected in the forest biome scores; (iii) the amplitude of the collapse of all the forest biome during the last millennium is remarkable and points to the major impact of the Medieval warm period in the deep tropics.

511 Our sensitivity experiment and inverse-vegetation modeling approach show that
512 atmopsheric CO_2 concentration unequally impact on vegetation due to different local
513 environments such as climates at each site. This study also suggests that the biome changes prior
514 to the Holocene resulted from both changes in the atmopsheric CO_2 concentration and climate;
515 the development and establishment of warm mixed forest from the xerophytic vegetation results
516 from increases in atmopsheric CO_2 concentration and near-surface air temperature. The
517 difference of local dryness also influences the biome distribution between the two sites, more
518 forest-type biome at Bambili and more grass/shrub-type biome at Rusaka. Finally, our climate
519 reconstruction proposes that the post-glacial climate in equatorial Africa may have been more
520 mesic than previous studies suggest.

521 **Acknowledgements**

522 This research was funded by the National Research Funding Agency in France (ANR-09-PEXT-
523 001 C3A) and the Belgian Federal Science Policy Office (BR/132/A1/AFRIFORD). Rusaka
524 pollen data were extracted from the African Pollen Database (http://fpd.sedoo.fr/fpd/) and
525 Bambili pollen data are available from the AML. We thank H. Chevillotte and S. Janicot for their
526 contribution. We are also grateful Patrick Bartlein and two anonymous reviewers for their
527 insightful comments on the manuscript. KI is supported by Labex L-IPSL and AML is supported
528 by CNRS.

529 **References**

530 Alley, R. B., 1997. *Holocene climatic instability; a prominent, widespread event 8,200 yr ago.*
531 Geology 25, 483–486.

Amaral, P. G. C., Vincens, A., Guiot, J., Buchet, G. , Deschamps, P., Doumnang, J.-C., Sylvestre, F., 2013. Palynological evidence for gradual vegetation and climate changes during the African Humid Period termination at 13°N from a Mega-Lake Chad sedimentary sequence. Climate of the Past 9, 223-241.

Anadón, J. D., Sala, O. E., Maestre, F. T., 2014. Climate change will increase savannas at the expense of forests and treeless vegetation in tropical and subtropical Americas. Journal of Ecology 102, 1363-1373.

Bazin, L., 2013. Carbon dioxide composite data on AICC2012 chronology. Doi:10.1594/PANGAEA.824893

Berger, A., Loutre, M. F., 1991. Insolation values for the climate of the last 10 million years. Quaternary Science Reviews 10, 297-317.

Bonnefille, R., Potts, R., Chalié, F., Jolly, D., Peyron, O., 2004. High-resolution vegetation and climate change associated with Pliocene Australopithecus afarensis. Proceedings of the National Academy of Sciences of the United States of America 101, 33, 12125-12129.

Bonnefille, R., Riollet, G., Buchet, G., Icole, M., Lafont, R., Arnold, M., Jolly, D., 1995. Glacial/Interglacial record from Intertropical Africa, high resolution pollen and carbon data at Rusaka, Burundi. Quaternary Science Reviews 14, 917-936.

Braconnot, P., Otto-Bliesner, B., Harrison, S., Joussaume, S., Peterchmitt, J.-Y., Abe-Ouchi, A., Crucifix, M., Driesschaert, E., Fichefet, T., Hewitt, C. D., Kageyama, M., Kitoh, A., Laine, A., Loutre, M.-F., Marti, O., Merkel, U., Ramstein, G., Valdes, P., Weber, S. L., Yu, Y., Zhao, Y., 2007a. Results of PMIP2 coupled simulations of the mid-Holocene and Last Glacial maximum e part 1: experiments and large-scale features. Climate of the Past 3, 261-277.

555 Braconnot, P., Otto-Bliesner, B., Harrison, S., Joussaume, S., Peterchmitt, J.-Y., Abe-Ouchi, A.,
556 Crucifix, M., Driesschaert, E., Fichefet, T., Hewitt, C. D., Kageyama, M., Kitoh, A., Laine,
557 A., Loutre, M.-F., Marti, O., Merkel, U., Ramstein, G., Valdes, P., Weber, S. L., Yu, Y.,
558 Zhao, Y., 2007b. Results of PMIP2 coupled simulations of the mid-Holocene and Last
559 Glacial maximum - part 2: feedbacks with emphasis on the location of the ITCZ and mid-
560 and high latitudes heat budget. Climate of the Past 3, 279-296.
561 Brncic, T.M., Willis, K.J., Harris, D.J., Telfer, M.W., Bailey, R.M., 2009. Fire and climate
562 change impacts on lowland forest composition in northern Congo during the last 2580
563 years from palaeoecological analyses of a seasonally flooded swamp. The Holocene 19,1,
564 79–89.
565 Brooks, A., Farquhar, G. D., 1985. Effect of temperature on the CO2/O2 specificity of ribulose-
566 1,5-bisphosphate carboxylase/oxygenase and the rate of respiration in the light. Planta 165,
567 397-406.
568 Cowling, S. A., Sykes, M. T., 1999. Physiological significance of low atmospheric CO_2 for
569 plant-climate interactions, Quaternary Research 52, 237-242.
570 de Menocal, P., Ortiz, J., Guilderson, T., Adkins, J., Sarnthein, M., Baker, L., Yarusinsky, M.
571 2000. Abrupt onset and termination of the African Humid Period: rapid climate responses
572 to gradual insolation forcing, Quaternary Science Reviews 19, 347–361.
573 Desjardins, T., Turcq, B., Nguetnkam, J.-P., Achoundong, G., Mandeng-Yogo, M., Cetin, F.,
574 Lézine, A.-M., 2013. $d^{13}C$ variations of soil organic matter as an indicator of vegetation
575 change during the Holocene in central Cameroon. C.R. Geosciences 345, 266-271.

576 Dupont, L. M., Jahns, S., Marret, F., Shi, N., 2000. Vegetation change in equatorial West Africa:
577 time-slices for the last 150 ka. Palaeogeography, Palaeoclimatology, Palaeoecology 155,
578 95-122.
579 Ehleringer, J. R, Cerling, T. E., Helliker, B. R., 1997. C4 photosynthesis, atmospheric CO_2 and
580 climate. Oecologia 112, 285-299.
581 Elenga H., Peyron O., Bonnefille R., Prentice I.C., Jolly D., Cheddadi R., Guiot J., Andrieu V.,
582 Bottema S., Buchet G., de Beaulieu J.-L., Hamilton A.C., Maley J., Marchant R., Perez-
583 Obiol R., Reille M., Riollet G., Scott L., Straka H., Taylor D., Van Campo E., Vincens A.,
584 Laarif F., Jonson H., 2000. Pollen-based biome reconstruction for southern Europe and
585 Africa 18,000 years ago. Journal of Biogeography 27, 621-634.
586 Friend, A. D., Woodward, F. I., 1990. Evolutionary and ecophysiological responses of mountain
587 plants to the growing season environment. Advances in Ecological Research 20, 59-124.
588 Food and Agricultural Organization of the United Nations (FAO), 1995. Digital Soil Map of the
589 World and Derived Soil Properties (Version 3.5), FAO, Rome, Italy.
590 Gasse, F., 2000. Hydrological changes in the African tropics since the Last Glacial Maximum,
591 Quaternary Science Reviews 19, 189–211.
592 Gasse, F., Chalié, F., Vincens, A., Williams, M. A. J., Williamson, D., 2008. Climatic patterns in
593 equatorial and southern Africa from 30,000 to 10,000 years ago reconstructed from
594 terrestrial and near-shore proxy data. Quaternary Science Reviews 27, 2316–2340.
595 Guiot, J., Torre, F., Jolly, D., Peyron, O., Boreux, J. J., Cheddadi, R., 2000. Inverse vegetation
596 modeling by Monte Carlo sampling to reconstruct palaeoclimates under changed
597 precipitation seasonality and CO2 conditions: application to glacial climate in
598 Mediterranean region. Ecological Modelling 127, 2-3, 119-140.

599 Guiot, J., Wu, H. B., Garreta, V., Hatte, C., Magny, M., 2009 A few prospective ideas on climate
600 reconstruction: from a statistical single proxy approach towards a multi-proxy and
601 dynamical approach. Climate of the Past 5, 4, 571-583.
602 Hély, C., Lézine, A.-M. and contributors, 2014. Holocene changes in African vegetation:
603 tradeoff between climate and water availability. Climate of the Past 10, 681-686.
604 Huang, Y. S., Street-Perrott, F. A., Perrott, R. A., Metzger, P., Eglinton, G., 1999. Glacial-
605 interglacial environmental changes inferred from molecular and compound-specific $\delta^{13}C$
606 analyses of sediments from Sacred Lake My. Kenya. Geochimica et Cosmochimica Acta
607 63, 1383-1404.
608 Izumi, K., 2014. Application of paleoenvironmental data for testing climate models and
609 understanding past and future climate variations. PhD Thesis, Universite of Oregon,
610 Eugene, USA.
611 Izumi, K., Bartlein, P. J., in revision. North American paleoclimate reconstructions for the last
612 glacial maximum using an inverse-modeling through iterative-forward-modeling (IMIFM)
613 approach applied to pollen data. Geophysical Research Letters.
614 Jolly, D., Harrison, S. P., Damnati, B., Bonnefille, R., 1998b. Simulated climate and biomes of
615 Africa during the late Quaternary: comparison with pollen and lake status data. Quaternary
616 Sciences Reviews 17, 629-657.
617 Jolly, D., Haxeltine, A., 1997. Effect of low glacial atmospheric CO_2 on tropical African
618 montane vegetation. Science 276, 786-788. doi:10.1126/science.276.5313.786
619 Jolly, D., Prentice, I. C., Bonnefille, R., Ballouche, A., Bengo, M., Brenac, P., Buchet, G.,
620 Burney, D., Cazet, J. P., Cheddadi, R., Edorh, T., Elenga, H., Elmoutaki, S., Guiot, J.,
621 Laarif, F., Lamb, H., Lézine, A.-M., Maley, J., Mbenza, M., Peyron, O., Reille, M.,

622 Reynaud-Farrera, I., Riollet, G., Ritchie, J. C., Roche, E., Scott, L., Ssemmanda, I., Straka,
623 H., Umer, M., Van Campo, E., Vilimumbalo, S., Vincens, A., Waller, M., 1998a. Biome
624 reconstructions from pollen and plant macrofossil data for Africa and the Arabian
625 peninsula at 0 and 6000 yrs. Journal of Biogeography 25, 1007-1027.
626 Kaplan, J. O., Bigelow, N. H., Prentice, I. C,. Harrison, S. P., Bartlein, P. J., Christensen, T. R.,
627 Cramer, W., Matveyeva, N. V., McGuire, A. D., Murray, D. F., Razzhivin, V. Y., Smith,
628 B., Walker, D. A., Anderson, P. M., Andreev, A. A., Brubaker, L. B., Edwards, M. E.,
629 Lozhkin, A. V., 2003. Climate change and Arctic ecosystems: 2. Modeling, paleodata-
630 model comparisons, and future projections. Journal of Geophysical Research-Atmospheres
631 108, D19. doi:10.1029/2002jd002559
632 Lebamba, J., Vincens, A., Maley, J., 2012. Pollen, vegetation and climate at Lake Barombi Mbo
633 (Cameroon) during the last ca. 33 000 cal yr BP: a numerical approach. Climate of the the
634 Past 8, 59-78.
635 Letouzey, R., 1968. *Etude phytogéographique du Cameroun*. P. Lechevalier ed., Paris 511p.
636 Letouzey, R., 1985. Notice de la carte phytogéographique du Cameroun au 1 : 500 000. Institut
637 de la Carte Internationale de la Végétation, Toulouse, France.
638 Lézine, A.-M., 2007. Postglacial Pollen Records of Africa. *In* Encyclopaedia of Quaternary
639 Sciences, **Scott A Elias ed.,** Elsevier. 4, 2682-2698.
640 Lézine, A.-M., Assi-Kaudjhis, C., Roche, E., Vincens, A., Achoundong, G., 2013a. Towards an
641 understanding of West African montane forest response to climate change. *Journal of*
642 *Biogeography* 40, 1, 183–196.

643 Lézine, A.-M., Hély, C., Grenier, C., Braconnot, P., Krinner, G., 2011. Sahara and Sahel
644 vulnerability to climate changes, lessons from paleohydrological data. Quaternary
645 Science Reviews 30, 21-22, 3001-3012.
646 Lézine, A.-M., Holl, A., Assi-Kaudjhis, C., Février, L., Lebamba, J., Vincens, A., Sultan, E.,
647 2013b Central African forests, human populations and climate during the Holocene. *C.R.*
648 *Geosciences* 345, 7-8, 327-335.
649 Lézine, A.-M., Watrin, J., Vincens, A., Hély, C., Contributors., 2009. Are modern pollen data
650 representative of west African vegetation? Review of Palaeobotany and Palynology 156,
651 265–276.
652 Loehle, C., 2007. Predicting Pleistocene climate from vegetation in North America. Climate of
653 the Past 3, 109-118.
654 Maley, J., 1996. The African rain forest: main characteristics of changes in vegetation and
655 climate from the upper Cretaceous to the Quaternary. *In:* Essays on the Ecology of the
656 Guinea-Congo Rain Forest *(*Alexander IJ*,* Swaine MD*,* Watling R *eds), pp.* 31–73*,*
657 *Proceedings of the Royal Society of Edinburgh 104B, Edinburgh.*
658 Maley, J., Brenac, P., 1998. Vegetation dynamics, paleoenvironments abd climatic changes in
659 the forest of West Cameroon during the last 28,000 years. Rev., Paleobot. & Palyno., 99,
660 157-188.
661 Marchant R., Hooghiemstra H., 2004. Rapid environmental change in African and South
662 American tropics around 4000 years before present: a review. Earth Science Reviews 66,
663 217-260.
664 Momo Solefack, M. C., 2009. Influence des activite´s anthropiques sur la végétation du Mont
665 Oku (Cameroun). PhD Thesis, Université de Picardie, Amiens, France.

New, M., Lister, D., Hulme, M., Makin, I., 2002. A high-resolution data set of surface climate over global land areas. Climate research, 21, 1-25.

Novello, A., Lebatard, A. E., Moussa, A., Barboni, D., Sylvestre, F., Bourlès, D.L., Paillès, C., Buchet, G., Decarreau, A., Duringer, P., Ghienne, J. F., Maley, J., Mazur, J.C., Roquin, C., Schuster, M., Vignaud, P., 2015. Diatom, phytolith, and pollen records from a $^{10}Be/^{9}Be$ dated lacustrine succession in the Chad basin: Insight on the Miocene–Pliocene paleoenvironmental changes in Central Africa. Palaeogeography, Palaeoclimatology, Palaeoecology 430, 85–103.

Prentice, I. C., Bondeau, A., Cramer, W., Harrison, S. P., Hickler, T., Lucht, W., Sitch, S., Smith, B., Sykes, M. T., 2007. Dynamic global vegetation modelling: quantifying terrestrial ecosystem responses to large-scale environmental change. In: Canadell, J. D., Pataki, E., Pitelka, L. F. (eds.), Terrestrial Ecosystems in a Changing World. Springer-Verlag, Berlin, pp.175-192.

Prentice, I. C., Harrison, S. P., 2009. Ecosystem effects of CO2 concentration: evidence from past climates. Clim Past 5, 297-307.

Prentice, I. C., Jolly, D., BIOME 6000 participants., 2000. Mid-Holocene and glacial-maximum vegetation geography of the northern continents and Africa. Journal of Biogeography 27, 507-519.

Prentice, I. C., Sykes, M. T., Lautenschlager, M., Harrison, S. P., Denissenko, O., Bartlein, P. J., 1993. Modelling global vegetation pattern and terrestrial carbon storage at the last glacial maximum. Global Ecol Biogeogr Lett, 3, 67-76.

Prentice, I. C., Webb, T., 1998. BIOME 6000: reconstructing global mid-Holocene vegetation patterns from palaeoecological records. Journal of Biogeography 25, 6, 997-1005.

689 Runge, J., 2002. Holocene landscape history and palaeohydrology evidenced by stable carbon
690 isotope (d13C) analysis of alluvial sediments in the Mbari valley (5°N/23°E), Central
691 African Republic. Catena 48, 67-87.
692 Sakata, T., Yokoi, Y., 2002. Analysis of the O_2 dependency in leaf-level photosynthesis of two
693 *Reynoutria japonica* populations growing at different altitudes. Plant, Cell and
694 Environment, 25, 65-74.
695 Stager, J. C., Mayewski, P. A., Meeker, L. D., 2002. Cooling cycles, Heinrich event 1, and the
696 desiccation of Lake Victoria. Palaeogeography, Palaeoclimatology, Palaeococlogy 183,
697 169-178.
698 Street-Perrot, F. A., Huang, Y. S., Perrott, R. A., Eglinton, G., Barker, P., Benkhelifa, L.,
699 Harkness, D. D., Olago, D. O., 1997. Impact of lower atmospheric carbon dioxide on
700 tropical mountain ecosystems. Science 278, 5342, 1422-1426.
701 Terashima, I., Masuzawa, T., Ohba, H., Yokoi, Y., 1995. Is photosynthesis suppressed at higher
702 elevation due to low CO_2 pressure. Ecology 76, 2663-2668.
703 Tierney, J. E., Russel, J. M., Huang, Y., Sinninghe Damsté, J. S., Hopmans, E. C., Cohen, A. S.,
704 2008. Northern hemisphere controls on tropical southeast African climate during the past
705 60,000 years. Science 322, 252-255.
706 Tierney, J.E., deMenocal, P.B. 2013. Abrupt shifts in Horn of Africa hydroclimate since the last
707 glacial maximum. Science 342, 843-846.
708 Troupin, G., 1982. Flore des plantes ligneuses du Rwanda. Institut national de la Recherche
709 scientifique, Butare747p.
710 Verschuren, D., Laird, K. R., Cumming, B. F., 2000. Rainfall and cdrought in equatorialeast
711 Africa during the past 1,100 years. Nature 403, 410-413.

712 Vincens, A., Bremond, L., Brewer, S., Buchet, G., Dussouillez, P., 2006. Modern pollen-based
713 biome reconstructions in East Africa expanded to southern Tanzania. Review of
714 Palaeobotany and Palynology 140, 187-212.
715 Vincens, A., Buchet, G., Servant, M., ECOFIT Mbalang collaborators., 2010. Vegetation
716 response to the « African Humid Period » termination in Central Cameroon (7°N) – new
717 pollen insight from lake Mbalang. Climate of the Past 6, 281-294.
718 Vincens, A., Lézine, A.-M., Buchet, G., Lewden, D., Le Thomas, A., Contributors., 2007.
719 African pollen database inventory of tree and shrub pollen types. Review of Palaeobotany
720 and Palynology 145, 135-141.
721 Vincens, A., Schwartz, D., Elenga, H., Reynaud-Farrera, I., Alexandre, A., Bertaux, J., Mariotti,
722 A., Martin, L., Meunier, J.-D., Nguetsop, F., Servant, M., Servant-Vildary, S., Wirrmann,
723 D., 1999. Forest response to climate changes in Atlantic Equatorial Africa during the last
724 4000 years BP and inheritance on the modern landscapes. Journal of Biogeography 26,
725 879-885.
726 Watrin, J., Lézine, A.-M., Hély, C., contributors., 2009. Plant migration and ecosystems at the
727 time of the "green Sahara", Comptes Rendus de l'Académie des Sciences – Géosciences,
728 341, 656- 670.
729 Weldeab, S., Schneider, R.R., Kölling, M., Wefer, G., 2005. Holocene African droughts relate to
730 eastern equatorial Atlantic cooling. Geology 33,981-984.
731 White, F., 1983. *The vegetation of Africa.* UNESCO, Paris, 384p.
732 Wu, H., Guiot, J., Brewer, S., Guo, Z., 2007a. Climatic changes in Eurasia and Africa at the last
733 glacial maximum and mid-Holocene: reconstruction from pollen data using inverse
734 vegetation modeling. Climate Dynamics 29, 211–229.

735 Wu, H., Guiot, J., Brewer, S., Guo, Z., Peng C., 2007b. Dominant factors controlling glacial and
736 interglacial variations in the treeline elevation in tropical Africa. Proceedings of the
737 National Academy of Sciences of the United States of America 104, 23, 9720-9724.